On the investigation of Fresnel and Fraunhofer diffraction patterns through various apertures.

Geri Nicka
School of Physics, University of Bristol.
(Dated: February 17, 2020)

1. INTRODUCTION

Diffraction patterns of electromagnetic waves through various apertures can be investigated by developing an appropriate computer simulation. Considering a square aperture of width x' and height y' and a screen with dimensions x and y at distance z from the aperture, diffraction patterns on the screen can be observed. At points where waves from the aperture are almost parallel, the Fraunhofer equation can be applied to model these diffraction patterns. More specifically, this arises for values of the Fresnel number which are significantly less than one [1]. The Fresnel number is defined as,

$$F = \frac{a^2}{z\lambda}, \tag{1}$$

where a is the aperture width, z the distance between the aperture and the screen and λ the incident wavelength. On the contrary, for Fresnel numbers greater than one, diffraction patterns alter, resulting in near-field or Fresnel diffraction [2].

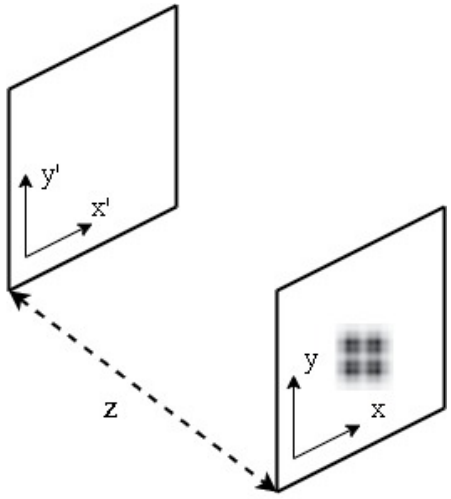

FIG. 1. Near-field diffraction from a square aperture.

Applying the Huygen-Fresnel principle [3], which considers the contribution in the electric field from multiple spherical wavelets along the aperture, the intensity of incident waves on the screen can be determined and used to model the near-field diffraction pattern for wavelengths much smaller than the distance between the aperture and the screen.

Under the assumption that waves are propagated parallel to the z coordinate and that the origin is taken to be at the aperture for $z = 0$, the electric field of the incident light $E(x, y, x)$ originating from an aperture of arbitrary shape is given by,

$$Q \iint_A \exp \frac{ik}{2z}[(x - x')^2 + (y - y')^2]\, dx'\, dy', \tag{2}$$

where $Q = kE_0/2\pi z$ and $k = 2\pi/\lambda$. The magnitude of the electric field in the screen squared is proportional to the intensity of the incident waves,

$$I(x, y, z) \propto \mid E^2(x, y, z) \mid . \tag{3}$$

In the present computer simulation, integral (2) is numerically solved for a square aperture area with the aim to visualise the near-field diffraction pattern in one and two dimensions and explore the effects of varying the distance to the screen and the aperture size. A significant extension to this investigation, is the adaptation of the computer program to simulate diffraction patterns through any arbitrary shape.

2. SIMPSON'S METHOD

The computer program developed focuses on Simpson's rule for numerical integration where the integrand can be approximated by a series of quadratics which involve three adjacent points. More explicitly, $N + 1$ values in a certain range are approximated using equally spaced subintervals. Its general form is,

$$\int_a^b f(x)dx = \frac{\Delta x}{3} \sum_{j=1}^{N/2} [f(x_{2j-2}) + 4f(x_{2j-1}) + f(x_{2j})] \tag{4}$$

where $\Delta x = \frac{b-a}{N}$ and $x_j = a + j\Delta x$. Simpson's method is substantially more accurate than the Trapezoidal Rule [3] and it is a frequent method of numerical integration unless other more sophisticated approaches,like the Tanh-Sinh Quadrature [4], which involve the change of variables are implemented.

3. PROGRAMMING METHODS

The fundamental structure of the code was the definition of the functions responsible for evaluating the one and two dimensional integrals with Simpson's Rule. Function **Simpson** was defined such that any general function **f** was accepted as an argument and its integral over a certain range was approximated implementing the Simpson method for one dimension.

In one dimension, the electric field $E(x, z)$ was simplified to be,

$$Q \int_{x_1'}^{x_2'} \exp \frac{ik}{2z}(x - x')^2 dx', \tag{5}$$

which was accepted as an argument for **Simpson** and evaluated the electric field for any given x in the screen coordinate. Using relation (3) an array of x values was initialized and substituted into equation (5) to plot the relative intensity in one dimension. In order to explore the effects of near field diffraction a user menu was structured such that the aperture and screen size and the distance z between them could be adjusted.

The diffraction pattern of a square aperture in two dimensions was visualised applying the same method as in one dimension twice by naming two arrays x and y and substituting them into a two dimensional array of intensity values for each pair (x, y). Integral (2) becomes separable for a square aperture and can be expressed as the product of two one dimensional integrals

$$Q \int_{x_1'}^{x_2'} \exp \frac{ik}{2z}(x - x')^2 dx' \int_{y_1'}^{y_2'} \exp \frac{ik}{2z}(y - y')^2 dy' \tag{6}$$

which was applied to obtain values for intensity in a two dimensional plane. The accuracy of the patterns generated depends on the steps in each range dx' and dy'. Images obtained at $100x100$ pixels were relatively clear but lacked detail in regions where intensity was reduced. It was found that at $1000x1000$ pixels significantly higher resolution images were generated, able to show low intensity features of the observed patterns.

Non-separable integrals which describe the area of any general shape of aperture could not be computed without further developments in the present computer simulation. As an extension, functions **Integration2DSimpson** and **E2DAnyShape** were defined. The former is responsible for performing the Simpson rule in the x and y axes and evaluates any integrand accepted as an argument for any arbitrary area. The latter is the product of the integrand and an array which identifies black and white pixels in an aperture image file. Waves passing through the aperture, which corresponds to the white area in the image, result in diffraction patterns unique for every shape. The final process of visualizing the patterns was executed using a loop within a loop in which values depending on the x and y coordinates on the screen are assigned to a two dimensional array of intensities.

4. RESULTS

In one dimension, the Fraunhofer diffraction pattern observed is the expected one for Fresnel numbers much less than one. The effect of changing the number of subintervals within the limits of integration N did not cause any changes in the

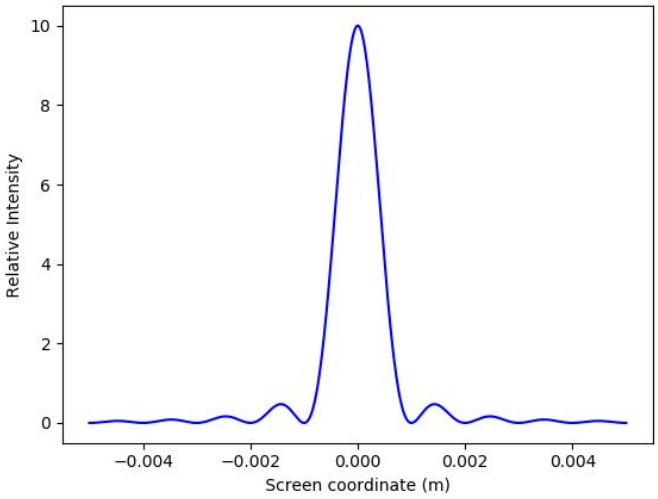

FIG. 2. Relative light intensity incident on screen. Parameters used were: $z = 2cm$, $x_2' - x_1' = 20\ \mu m$, $k = 6.28 * 10^6\ 1/m$ and $N = 100$.

shape of the relative intensity curve. Increasing the width of the square aperture, it was observed in Figure 3 that the central maximum of intensity increased and turned narrower while conserving the same shape. The underlying physics behind this effect is that as more light passes though the aperture the electromagnetic flux incident on the screen increases. Opposite results were examined by increasing the distance between the aperture and the screen. At larger distances light intensity is weaker while the peak becomes broader due to less incident radiation on the screen per unit time as shown in Figure 4.

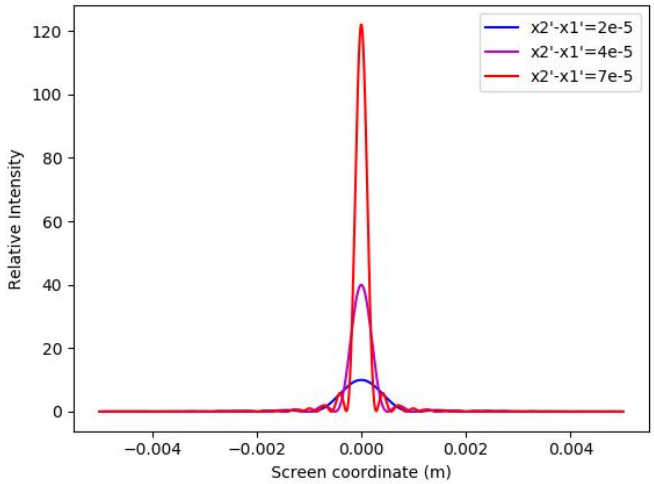

FIG. 3. Relative light intensity incident on screen for different aperture widths. Parameters used were: $z = 2\ cm$, $k = 6.28 * 10^6\ 1/m$ and $N = 100$.

Near- field diffraction can be observed by choosing a combination of the aperture area, wavelength and distance to the screen such that the Fresnel number is greater than one. More

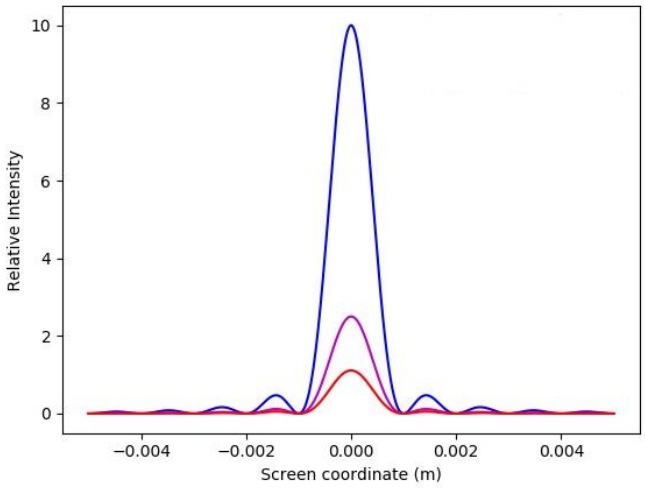

FIG. 4. Relative light intensity incident on screen with varying z. Parameters used: $x_2' - x_1' = 20\ \mu m$, $k = 6.28 * 10^6\ 1/m$ and $N = 100$. Blue(2 cm), magenta(4 cm) , red (8cm).

distinct features of these diffraction patterns can be investigated if the Fresnel number is significantly greater than one. It was found that a higher number N was needed to accurately portray a correct near-field diffraction pattern. The periodic

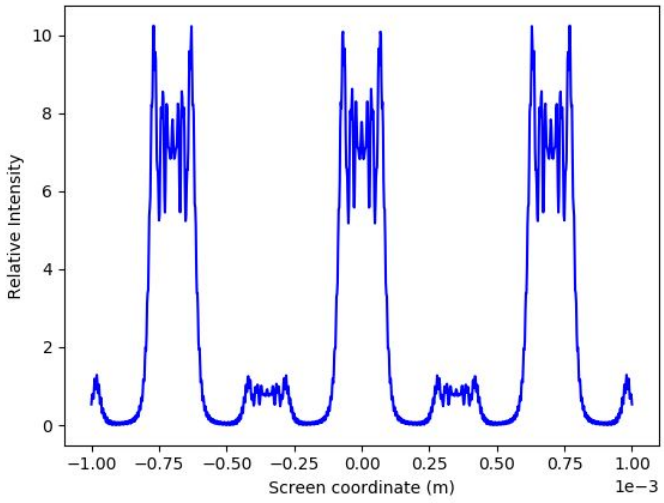

FIG. 5. Misleading Fresnel diffraction pattern caused by a small number N. Parameters used were: $x_2' - x_1' = 200\ \mu m$, $k = 6.28 * 10^6\ 1/m$ and $N = 100$.

curve in Figure 5 is not a valid representation of what is physically happening during Fresnel diffraction and is an artefact of the Simpson rule. This is due to the fact that the Simpson method is inaccurate for functions that evolve rapidly. To fix this, a larger number N is used and more quadratic approximations are performed. The result of a graph illustrating actual Fresnel Diffraction is shown in Figure 6. This is also verified by calculating the Fresnel number for this particular graph, which was approximately 35.

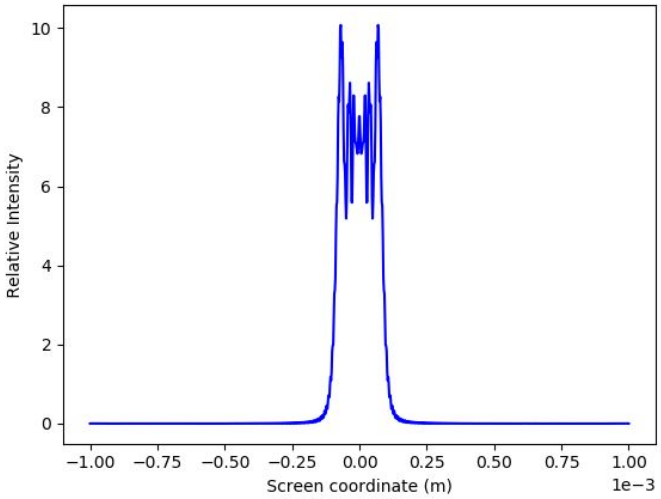

FIG. 6. Correct Fresnel diffraction pattern obtained using a large value for N. Parameters used were: $z = 1.4\ mm$, $x_2' - x_1' = 200\ \mu m$, $k = 6.28 * 10^6\ 1/m$ and $N = 100$.

The relative intensity for Fraunhofer diffraction in two dimensions is shown in Figure 7. The colour intensity on the plot indicates the intensity peaks with the center one being the central maximum. A high resolution image was achieved by a $1000x1000$ pixel resolution.

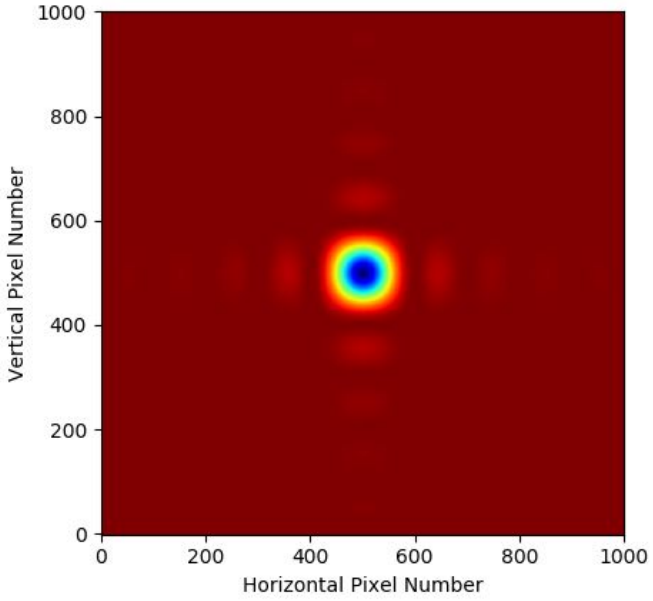

FIG. 7. Relative intensity for Fraunhofer Diffraction in two dimensions. Parameters used were: $z = 2\ cm$, $x_2' - x_1' = y_2' - y_1' = 20\ \mu m$, $k = 6.28 * 10^6\ 1/m$ and $N = 100$.

The generated image in Figure 7 is a clear representation of the Fraunhofer diffraction pattern from a square aperture. Intensity is maximum at the center of the image (dark blue) and reduces away from it (light red).

Visualising Fresnel diffraction in two dimensions is a challenge as it must be ensured that the Fresnel number is adjusted to be much greater than one and N must be large enough for the Simpson method to be efficient. Axes in Figure 8 were omitted to emphasise on clarity. Pixel resolution remains $1000x1000$ and N for the plots on the left and right is 10 and 100 respectively.

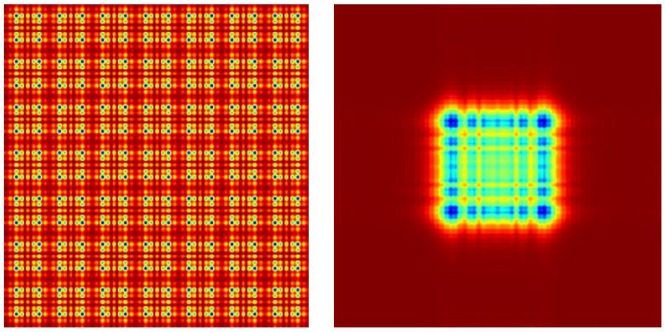

FIG. 8. Misleading Fresnel diffraction due to small N (left) and actual Fresnel diffraction using large N (right). Parameters used were: $z = 1.4\ mm$, $x_2' - x_1' = y_2' - y_1' = 200\ \mu m$ and $k = 6.28 * 10^6\ 1/m$ with $N = 10$ (left) and $N = 100$ (right) .

Further discussion of the results obtained for Fraunhofer and Fresnel diffraction in one and two dimensions will thoroughly analyse the physical reasons for which misleading images were generated.

The adaptation of the program to visualise diffraction patterns from any aperture shape resulted in certain images which are worth presenting in this report. Such shapes include single and multiple slits of different shapes all of which have a type of geometric symmetry.

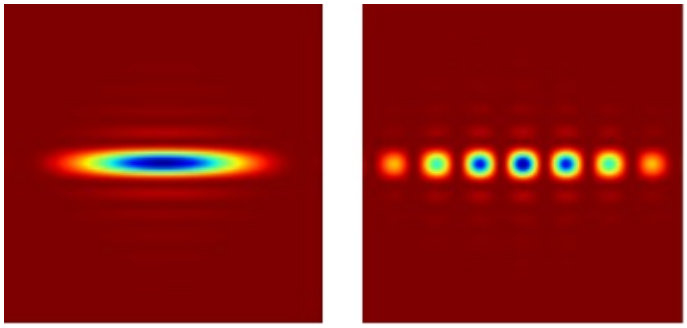

FIG. 9. Diffraction patterns of single slit (left) and double slit (right) apertures.

The diffraction patterns obtained in Figure 9 are for a single and double slit on the left and right respectively. The resolution used in the case of non-rectangular or square apertures was $500x500$ solely for clarity purposes. A user attempt to obtain these images with such a high resolution would take time to process from the computer as the Simpson rule is executed in two dimensions rather than one. However, the general trends of the pattern can be clearly observed by a $50x50$ resolution in under one minute. In addition, an aperture of two aligned circles and another one of three circles forming a triangle exhibited most interesting diffraction patterns as shown in Figure 10.

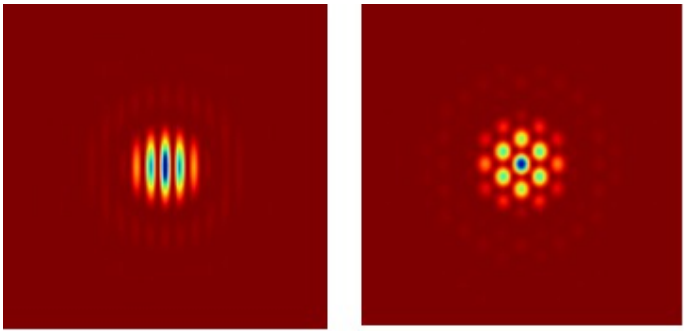

FIG. 10. Diffraction patterns of two aligned circles (left) and three circles forming a triangle (right).

The diffraction patterns obtained with the extended method were compared to the work of others [5] who have previously attempted to visualise patterns from such apertures to ensure the program was functioning properly.

5. DISCUSSION

The variations in diffraction patterns caused by increasing the size of the aperture can be analysed by considering the angle ϕ at which the first zero of the pattern emerges with respect to the aperture width a and the wavelength λ for a square or rectangular aperture given by,

$$sin\phi = \frac{\lambda}{a}. \tag{7}$$

Thus increasing or decreasing the aperture width causes a decrease or increase in the angle ϕ of the first minimum which is the constraint of the spread of the wave.

Intensity depends on the distance between the aperture and the screen in a simple manner. As distance is increased electromagnetic radiation spreads more around the screen resulting in images with a broad maximum and less or none subsequent maxima. On the other hand reducing the distance provides a larger area for additional maxima. These effects are shown in Figure 4.

Fresnel diffraction produces diffraction patterns which seem to be periodic as shown in Figure 5 and 8 (left). This is a misleading effect of the small number of subintervals N used by Simpson method to approximate the curve. To compensate for this, a significantly larger N is required to effectively visualise near-field effects as in Figures 6 and 8 (right).

It was discovered that near-field patterns do not appear to have the same kind of symmetry as in the far-field patterns as seen in Figure 11. Such an example is the near and far field diffraction pattern of a triangular aperture. As a three-fold

symmetric structure, it will show three-fold diffraction symmetry in the near-field but will exhibit six-fold symmetry in the far-field since three-fold rotation and centre of symmetry are involved. The reason for the centre of symmetry is attributed to the fact that, in the far field, the diffraction pattern is identical to the fourier transform of the convolution of the aperture with itself [6].

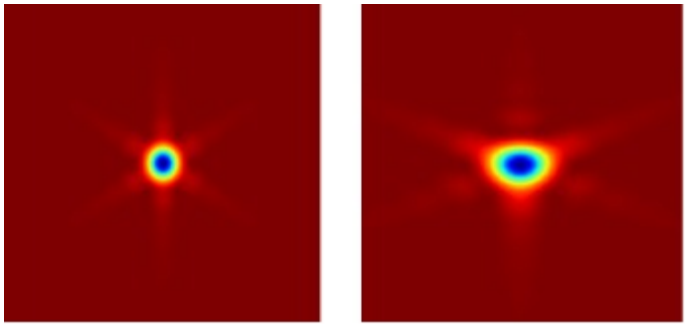

FIG. 11. Diffraction patterns of a triangular aperture in the far-field (left) and in the near-field (right) indicating the different types of symmetry.

A significant improvement to the program would be the approach of other methods of numerical integration such as the adaptive Simpson method. This approach exploits the estimate of the error arising from Simpson's rule and divides the range of integration in half for each step while applying the Simpson method twice [7]. This technique is deemed much more efficient than the traditional Simpson method as it evaluates less functions in regions which are approximated by cubic functions.

Moreover, vectorising functions instead of using iterative loops would substantially decrease the time elapsed to generate two dimensional plots without consuming a lot of processing power.

To render the comparison between the peaks in the plots of relative intensity more definite, three dimensional plots could have been generated in which features of the investigated diffraction patterns would be described completely.

Overall, the programming methods implemented were aimed to develop a time efficient algorithm which would model near and far field diffraction patterns as accurately as possible by adjusting the parameters of the problem accordingly and minimizing errors. Comparing the present work in this report to past attempts of other simulations it is concluded that the results obtained were accurate to a high degree and that the suggested improvements can render future simulations even more promising.

[1] Born, M.; Wolf, E. (2000). Cambridge U Press (ed.). Principles of optics. - 7th expanded ed. p. 486.

[2] Optics, Francis Weston Sears, p. 248ff, Addison-Wesley, 1948.

[3] "Huygens' Principle". MathPages. Retrieved 2017-10-03.

[4] Bailey, David H, Karthik Jeyabalan, and Xiaoye S. Li, "A comparison of three high-precision quadrature schemes". Experimental Mathematics, 14.3 (2005).

[5] G. Harburn, C.A. Taylor, T.R. Welberry, "Atlas of Optical Transforms ".

[6] Bracewell, R. N. (2000), The Fourier Transform and Its Applications (3rd ed.), Boston: McGraw-Hill.

[7] J.N. Lyness (1969), "Notes on the adaptive Simpson quadrature routine", Journal of the ACM, 16 (3): 483–495.